

**Original Research Article****Preparation and biomineralization of injectable hydrogel composite based chitosan-tetronic and biphasic calcium phosphate nanoparticles****Abstract**

In this study, a hydrogel composite was enzymatically prepared with rapid gelation time from tyramine-tetronic-conjugated chitosan and biphasic calcium phosphate (BCP) nanoparticles. The compressive stress of the hydrogel composite was reached at  $591 \pm 20$  KPa with 10wt% of BCP loading. Degradation study of the material showed 20% of weight loss after 4 weeks. *In vitro* study with MG 63 osteoblast cell evidenced that the cells were well-attached on hydrogel composite surfaces. Biomineralization on the hydrogel composites surfaces was well-observed after soaking for 14 days in simulated body fluid (SBF) solution. The obtained results indicated that the hydrogel composite could be an injectable potential material for bone regeneration.

**Key words**

Biomineralization, injectable, hydrogel composite, BCP nanoparticles, bone regeneration

**Introduction**

Recently, use of bioactive hydrogel scaffolds has been paid much attention in bone regeneration. The hydrogel scaffolds have highly porous 3D structure which creates a microenvironment for cell encapsulation, allowing nutrients and metabolites to diffuse to and from cells. However, most polymeric hydrogels do not occur a biomineralization which can be evaluated via formation of native apatite nanocrystals in SBF). Addition of an inorganic phase can produce a biomineralizable composites [1, 2]. Beside that the degradation of the hydrogel network also affects to the replacement by new bone formation, thus increases mechanically stability [3]. It is also well-known that the degradation times and mechanical properties of organic – inorganic composite materials are relevant and they can be controlled by the concentration of inorganic phase adding [4, 5]. In the presence of the loaded inorganic phase, the composites could promote nucleation and subsequent proliferation of calcium phosphate crystals that is often known as the capacity of a specific class of bone-substituting material to induce calcification [1]. This is an essential requirement for artificial material to generate to bonelike apatite and living bone. It also helps to neutralize pH caused by by-products, thus minimizing excessive inflammation around the implantation site [6, 7]. The

34 interactions between biological activity and its surrounding environment cause this  
35 precipitation [8]. Moreover, the loaded inorganic phase could provide cell adhesion sites for  
36 enable integration with surrounding bone tissue [9, 10]. There are many sources of inorganic  
37 phases, but one of the most commonly used calcium phosphate ceramic is BCP (mixture of  
38 hydroxyapatite and  $\beta$ -tricalcium phosphate) nanoparticles [11-13]. The nanoparticles have  
39 been utilized as inorganic phase for loading in several kinds of composite for bone  
40 regeneration.

41 This work focused on the preparation of hydrogel composite from chitosan derivative  
42 and BCP nanoparticles and evaluated its biomineralization via the formed apatite precipitate.  
43 Other features of hydrogel composite have also been studied to prove that this kind of  
44 material can be applied in bone regeneration.

#### 45 **Materials and methods**

46 Chitosan (Low Mw), p-nitrophenyl chloroformate (NPC), tyramine (TA) were  
47 purchased from Acros Organics. HRP (type VI, 298) was purchased from Sigma-Aldrich.  
48 Calcium chloride and trisodium phosphate were purchased from Merck, Germany. Tetronic  
49 1307 (Te, MW=18,000) was obtained from BASF. For the in vitro study, Fetal bovine serum  
50 (FBS), penicillin streptomycin antibiotic (PS), 3-[4,5-dimethylthiazol-2-yl]-2,5  
51 diphenyltetrazolium bromide (MTT) solution, and trypsin-EDTA were purchased from Gibco,  
52 Carlsbad, CA. MG-63 osteoblast cells were derived from rabbit osteosarcomas.

#### 53 *Preparation of BCP*

54 BCP NPs were synthesized by using an ultrasonic associated process as below  
55 formulation. Calcium chloride ( $\text{CaCl}_2$ ) were dissolved in 1.5 L distilled water and trisodium  
56 phosphate ( $\text{Na}_3\text{PO}_4$ ) were dissolved in 2.5 L distilled water with molar ratio of  $\text{Ca/P} = 1.57$ .  
57  $\text{CaCl}_2$  solution was put in an ultrasonic bath then adjusted pH 7 after that  $\text{Na}_3\text{PO}_4$  solution  
58 was also put in the ultrasonic bath. The reaction was occurred in 12 hours at  $50^\circ\text{C}$  to obtain a  
59 white suspension. The precipitate was washed thoroughly with distilled water and filtered  
60 before it was dried in an oven at  $70^\circ\text{C}$ . Finally, the calcination was carried out at  $750^\circ\text{C}$  in air  
61 [11, 13].

#### 62 *Preparation of TTeC copolymer*

63 TTeC copolymer was prepared as previously described [14]. The process to produce  
64 tetronic-grafted chitosan containing TA moieties is the combination of three synthetic

65 reactions without using any organic solvent to purify [14]. Briefly, the hydroxyl groups of  
66 tetronic were activated by NPC, then TA was partially added to conjugate into the activated  
67 product and the remaining moiety of tetronic-TA grafted onto chitosan to produce TTeC  
68 copolymer.

#### 69 *Preparation of hydrogel and gel composite*

70 *Preparation of hydrogel:* 40mg TTeC was dissolved in 260  $\mu$ L phosphate buffered  
71 saline (PBS) solution pH 7.4, and then, equally separated into two ependroff tubes. The PBS  
72 solutions of HRP (50  $\mu$ L of 0.2 mg/ml) and H<sub>2</sub>O<sub>2</sub> (50  $\mu$ L of 0.2% wt/vol ) were separately  
73 supplemented to each tube. TTeC hydrogel was immediately formed by mixing the  
74 solutions of 10% wt/wt polymer.

75 *Preparation of hydrogel composite:* Preparation of the TTeC/BCP hydrogel  
76 composites was done with same protocol in which BCP NPs (5 and 10% wt/wt) were added  
77 to two precursor copolymer solutions.

78 *Gelation time of the hydrogel or hydrogel composite:* The test tube inverting method  
79 was used to determine the gelation time. The solution was observed by inverting the vial and  
80 the gelation time was recorded when the solution stopped flowing. It was studied when the  
81 concentration of HRP was changed and the concentration of H<sub>2</sub>O<sub>2</sub> was kept at constant.

#### 82 *Characterizations*

83 The morphology and microstructure of the synthesized BCP powder was investigated  
84 by using FESEM (JSM-635F, JEOL). Compressive tests of the hydrogel composites were  
85 performed on a Universal Testing Machine (Unitech TM, R&B, Korea). To investigate the  
86 components of the hydrogel composite, the samples were analyzed via XRD (D8/Advance,  
87 Bruker, UK) with CuK $\alpha$ , ( $\lambda=1.5406$  Å) as a radiation source over the  $2\theta$  range of 10 - 60°.  
88 Water uptake of the hydrogels was determined by using the gravimetric method. The  
89 hydrogel composites were lyophilized and weighed ( $W_0$ ). These lyophilized hydrogels were  
90 immersed in 10 mL SBF solution at 37<sup>0</sup>C for 2 days to reach equilibrium swelling. Surface  
91 water was removed and the samples were weighed ( $W_s$ ). The water content in these  
92 lyophilized hydrogels was expressed by using the following equation:  $\frac{W_s - W_0}{W_0} \times 100\%$ . The  
93 degradation of hydrogel composites was studied in PBS. The hydrogel composites were  
94 lyophilized and weighed ( $W_0$ ). These lyophilized hydrogels were immersed in 10 mL PBS  
95 solution at 37<sup>0</sup>C. After regular time intervals, surface water was removed from the samples

96 and washed with deionized water to remove the soluble inorganic salt then weighted (Wt)  
97 after lyophilization. The percentage of weight loss is calculated to evaluate the degradation of  
98 hydrogel and gel composite as following formula:

99 
$$\text{Weight loss (\%)} = \frac{W_o - W_t}{W_o} \times 100\%$$

#### 100 *Cell proliferation study*

101 Firstly, MG-63 cells ( $5 \times 10^4$ ) seeded onto the UV-sterilized samples in 24-well plates  
102 for incubation, and came up with washing step by PBS for three times. The cell nuclei were  
103 counterstained with 20 mg/mL DAPI for 10 min at room temperature, the sample was then  
104 washed 3 times with 1X PBS. Finally, confocal laser scanning microscope (FV10i-W) was  
105 used to observe the stained cells on hydrogel composites after 5 days of cell seeding.

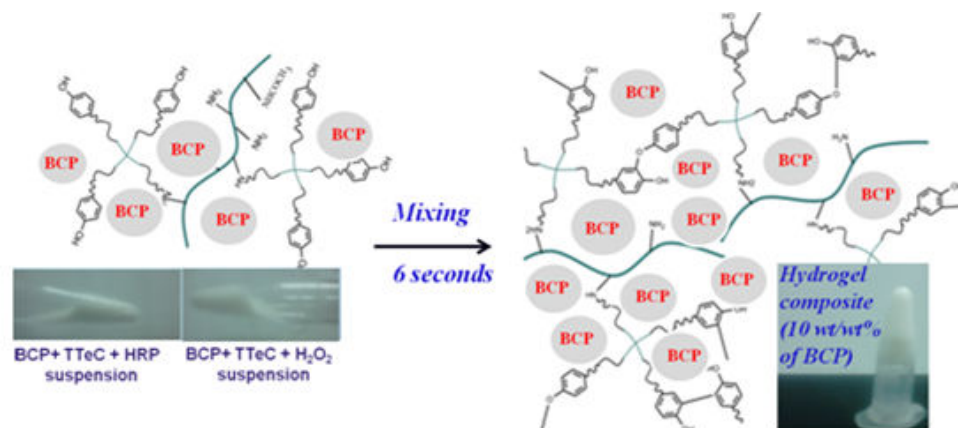
#### 106 *Biom mineralization evaluation*

107 To study the possible precipitate phase conversion, hydrogel composite samples  
108 immersed in a SBF buffer solution (pH 7.4). TTeC/BCP hydrogel composite was prepared  
109 and then lyophilized. Lyophilized hydrogel composite was cut to observe spongy surface then  
110 recorded its weight. Hydrogel composite was collected after 7 and 14 days of soaking in SBF  
111 and then washed with deionized water to remove the soluble ionorganic salt then weight (Wt)  
112 after lyophilization to confirm the decomposition of hydrogel composite. Finally, hydrogel  
113 composite was characterized by SEM, EDS and XRD.

## 114 **Results and discussion**

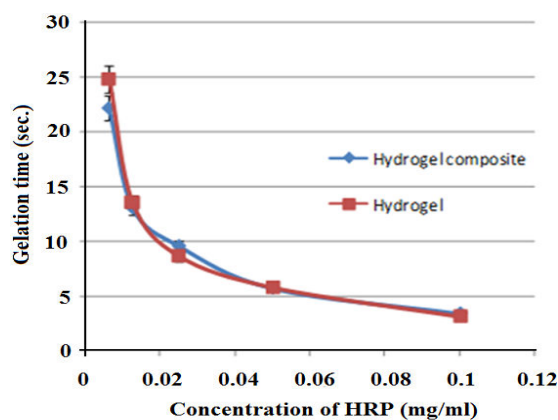
### 115 *Characterizations of hydrogel composite*

116 Figure 1 demonstrates in situ formation of hydrogel composite from two suspensions  
117 of BCP NPs and TTeC polymer in the presence of HRP enzyme. The gelation time of the  
118 TTeC/BCP hydrogel composites depended on concentration of HRP and  $H_2O_2$  (Figure 2). A  
119 change in HRP concentration with minimal supply of  $H_2O_2$  could result in reducing the  
120 gelation time due to the production of more phenolic radicals in the TTeC polymer solution.  
121 The minimal amount of the used  $H_2O_2$  could be easily determined by evaluation phenolic  
122 content in the polymer solution. With the high concentration of HRP (0.1 mg/ml), it took  
123 about 3 seconds to form the hydrogel composite and when the concentration of HRP was 0.05  
124 mg/ml, it took about 6 seconds to form hydrogel composite.



125  
126

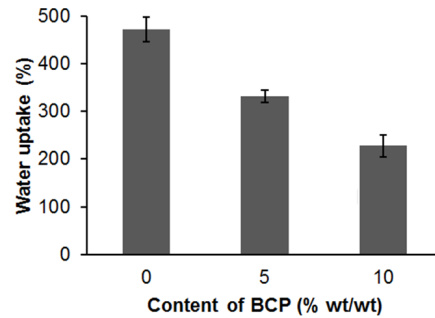
Figure 1. Formation of TTeC/BCP hydrogel composite



127

128 Figure 2. Effect of HRP concentration with feeded 0.05 wt% of H<sub>2</sub>O<sub>2</sub> on gelation time of  
129 TTeC hydrogel and TTeC/BCP hydrogel composite at 10% wt/wt polymer in solution

130 Water uptake of scaffold is related to its (their) ability to absorb body fluid and  
131 transfer cell nutrients and metabolites and is one of the most important properties of  
132 biomaterials. Figure 3 shows the water utilization by hydrogel composites. Both TTeC and  
133 their hydrogel composites could absorb water more than their own weight around 200%. The  
134 water uptake of TTeC-BCP hydrogel composite with 0, 5, and 10 wt% BCP was  $472.28 \pm 15$ ,  
135  $331.48 \pm 14$ , and  $228.35 \pm 14\%$  respectively. The water uptake decreased with an increase in  
136 the content of BCP NPs, that means the water uptake increased with increasing the  
137 concentration of TTeC polymer matrix. It can be explained by the hydrophilicity of the  
138 chitosan polymer matrix for the absorption of the body fluid that could have resulted in the  
139 more concentration of polymer matrix, the higher water retention [15, 16]. Moreover,  
140 released phosphate ions from BCP play a role as a crosslinker for chitosan network that  
141 increased the crosslinking density resulting in reducing water uptake of the composite [17]



142

143

Figure 3. Water uptake of hydrogel composite at different content of BCP

144

145

146

147

148

149

150

151

152

153

154

155

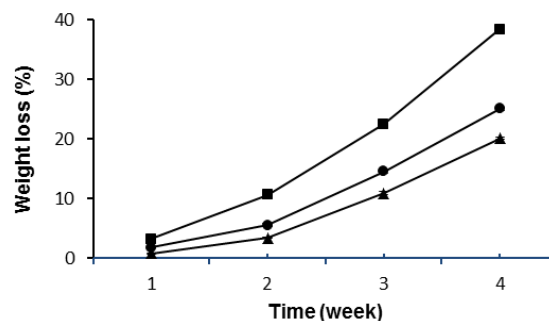
156

157

158

159

Degradation behavior of scaffolds plays an important role in tissue regeneration because scaffolds create and maintain a space for cell attachment and proliferation. The hydrogel composites should be maintained for a suitable time to replacement of new tissue. The degradation of the hydrogel composites was investigated by examining the weight loss of the hydrogels as a function of incubation time in PBS at 37<sup>0</sup>C. Figure 5 shows the degradation profiles of the TTeC/BCP hydrogel composites with different content of BCP NPs. Degradation of the hydrogel composites was maintained for over 1 month. The degradation of the TTeC/BCP hydrogel composites increased mass losses with increase in the polymeric matrix content. After 4 weeks, the weight loss ratios of the hydrogel composite containing 0 wt/wt%, 5 wt/wt% and 10 wt/wt% BCP NPs were 38%, 25% and 20% respectively. The degradation behavior of hydrogel composites was affected by adding of BCP NPs. It could be explained by the interaction between the released ions from BCP NPs and chitosan polymeric matrix. The NH<sub>2</sub>. OH groups of chitosan and OH group of HAp in BCP NPs have hydrogen bonding as well as the chelation between NH<sub>2</sub> group and Ca<sup>2+</sup> [17]. The degradation of hydrogel composite could be significant for growth of bone cells and new bone replacement [15, 16].



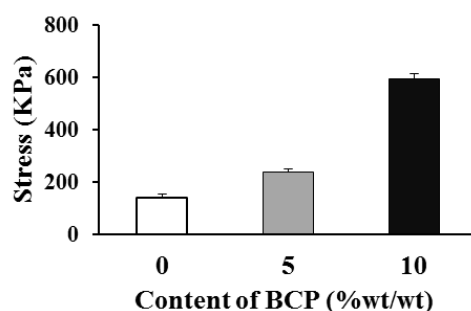
160

161

162

Figure 4. Weight ratios of TeTC/BCP hydrogel composites depending on content of BCP) ■ 0 wt/wt% BCP, ● 5 wt/wt% BCP, ▲ 10 wt/wt% BCP.

163 The compressive strength values of the TTeC/BCP hydrogel composites were  
164 determined  $138.7 \pm 15.9$ ,  $235.3 \pm 15.3$ , and  $591.7 \pm 19.5$  KPa for 0, 5, 10 % (wt) of the  
165 loaded BCP NPs, respectively (Figure 4). The compressive strength of the hydrogel  
166 composites was increased with increment in amount of the feed BCP NPs. This could be  
167 explained that incorporation of an inorganic reinforcing phase and interface adhesion of BCP  
168 particles within the hydrogel resulting in reinforcing of the polymer matrix. Moreover, the  
169 chemical interaction between the  $\text{NH}_2$  group of chitosan and OH group of HAp in BCP  
170 provided interfaces between polymer matrix and BCP particles [18-20]. Then, addition BCP  
171 into scaffolds improved the compressive strength of the composites.

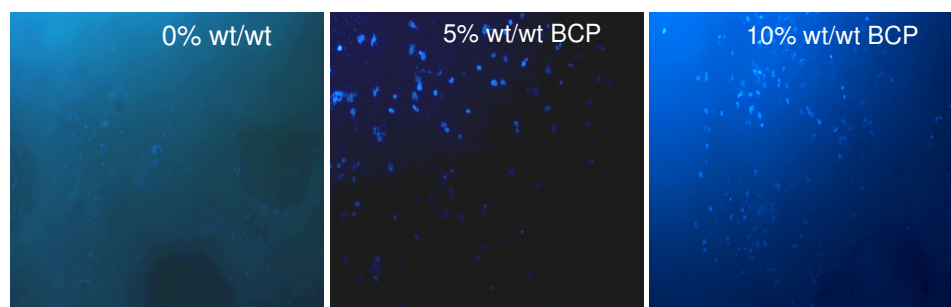


172

173 Figure 5. Compressive strength of the TTeC-BCP hydrogel composites.

#### 174 *Biocompatibility of the hydrogel composite*

175 DAPI-stained cell attachment on hydrogel composites was observed via fluorescence  
176 microscopy. The nuclei of the cells were blue after staining. The immunostained images  
177 exhibited a well attachment and proliferation of the MG-63 osteoblast cells on the surface of  
178 the hydrogel composites. After 5 days of incubation, cells were well-adhered on surface of  
179 the composites, more cells were observed on the TeTC/BCP hydrogel composite with higher  
180 BCP content. This great surface adherence was due to a high biocompatibility of hydrogel  
181 combined with effective characteristics of BCP such as rough surface creation the roughness  
182 surface and positive influence of calcium phosphate on the behavior of osteoblast cells,  
183 leading to enhanced cellular attachment [21, 22]. Viability and cell adhesion data confirmed  
184 that hydrogel composites are biocompatible.



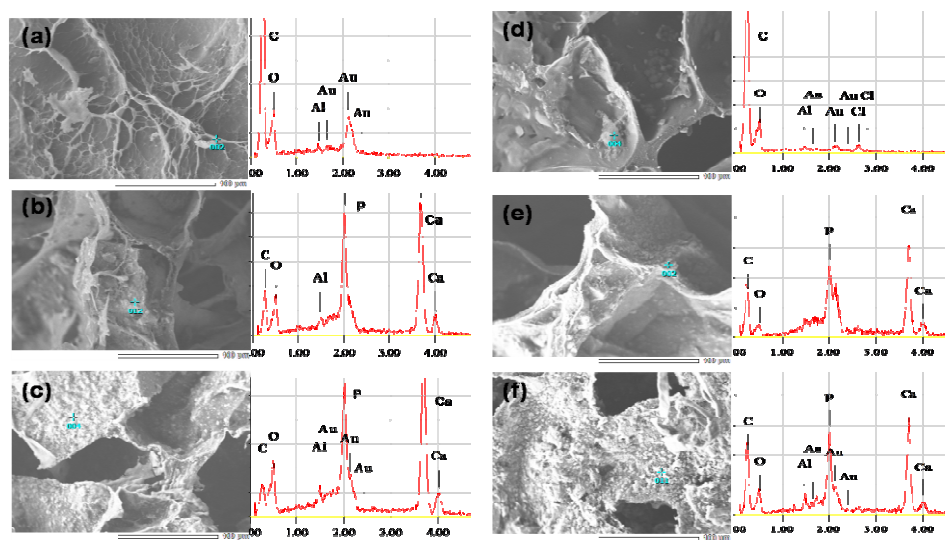
185

186 Figure 6. Confocal images of osteoblast cell MG-63 adhesion on TTeC/BCP hydrogel  
187 composites with different content of BCP after 5 days of incubation

### 188 *Biom mineralization of the hydrogel composite*

189 Biom mineralization study was used to predict the bioactivity of biomaterial in vivo  
190 study such as bone-bonding ability of bioactive materials. This mean, the apatite layer bond  
191 the biomaterial and the living bone [22, 23]. For hydrogel composite, mineralization behavior  
192 could be observed the apatite forming ability when samples were immersed in SBF for  
193 various periods of time. Figure 7 shows SEM micrographs of the surface morphology of  
194 hydrogel composites on which nucleation and growth of the precipitated-phase nanocrystals  
195 are visible on the surface of samples after 7 and 14 days. Figure 7(a) and (d) showed no  
196 apatite formation on surface of the TeTC hydrogel after 7 and 14 days of immersion in SBF.  
197 In contrast, the TeTC/BCP hydrogel composites were able to form the apatite layer when  
198 were being soaked in SBF. After incubation in SBF for 7 days, numerous tiny granular  
199 apatite particles were deposited on the hydrogel composite surfaces. Increasing the BCP  
200 content could result in forming more apatite crystals (Figure 7 (b), (c) and (e), (f)). The  
201 mineralization also increased with increasing immersion time. The results indicate that BCP  
202 enhanced the apatite forming ability on composites. BCP particles act as apatite nucleation  
203 sites, and then the apatite nuclei could grow by consuming the calcium and phosphate ions in  
204 the surrounding environment. Hence, the formation of apatite is more efficiently on the  
205 composite with higher content of BCP. The apatite precipitation through SBF test is a  
206 consequence of a dissolution and precipitation process. BCP in the composite gradually  
207 dissolves and releases calcium and phosphate ions which are beneficial to apatite formation.  
208 Moreover, the hydroxyl and phosphate unit in HAp, TCP crystal structure reveal negative  
209 charge of BCP particle surface when immersed in SBF. This negative charge attracted the  
210 positive calcium ions in SBF to form rich calcium surface, which interacts with the negative  
211 phosphate ions in SBF. As consequence, calcium and phosphate ions migrated to surface of  
212 hydrogel composite that induced the apatite precipitation [24-26]. EDS results in Figure 7

213 indicate that the precipitates on surface of TeTC/BCP hydrogel composite are calcium,  
 214 phosphorus and oxygen due to the composing element of apatite, which could be further  
 215 confirmed by XRD analysis (data not shown here). No new peaks appeared after immersion  
 216 in SBF was observed in XRD data. Hence, the precipitation on the surfaces of hydrogel  
 217 composites is apatite.



218  
 219 Figure 7. SEM micrograph and EDS profile of the composites without BCP NPs (a, d), with  
 220 5% BCP NPs (b, e) and with 10% BCP NPs (c, f) after soaking in SBF 7 and 14days.

221

## 222 Conclusions

223 Injectable polymer-grafted TeTC-BCP hydrogel composites prepared successfully. The  
 224 obtained results indicated that water absorbance, degradation behavior, compressive strength  
 225 and cell attachment as well as biomineralization of the hydrogel gels are dependent on the  
 226 content of BCP. Especially, the ability of forming apatite as well as cell proliferation of  
 227 hydrogel increased with higher content of BCP because BCP has positively influences on the  
 228 behavior of osteoblast cells and biomineralization process. These composite hydrogels have  
 229 the advantages of large amount of water absorbance, good mechanical strength, and suitable  
 230 degradation time, all of which are important to the regeneration of new bone tissue. TeTC-  
 231 BCP hydrogel composites could be promising materials for bone regeneration.

232

233

234

235

236 **References**

- 237 1. Gkioni K., Leeuwenburgh S.C., Douglas T.E., Mikos A.G., and Jansen J.A., Mineralization  
238 of hydrogels for bone regeneration, *Tissue Eng. Part B Rev.*, 2010; **16**, 577-85.
- 239 2. Pek Y.S., Kurisawa M., Gao S., Chung J.E., and Ying J.Y., The development of a  
240 nanocrystalline apatite reinforced crosslinked hyaluronic acid-tyramine composite as an  
241 injectable bone cement, *Biomater.*, 2009; **30**: 822-28.
- 242 3. Alsberg E., Kong H.J., Hirano Y., Smith M.K., Albeiruti A., and Mooney D.J., Regulating  
243 bone formation via controlled scaffold degradation, *J. Dent. Res.*, 2003; **82**: 903-8.
- 244 4. Rezwan K., Chen Q.Z., Blaker J.J., and Boccaccini A.R., Biodegradable and bioactive  
245 porous polymer/inorganic composite scaffolds for bone tissue engineering, *Biomater.*,  
246 2006; **27**: 3413-31.
- 247 5. Ara M., Watanabe M., and Imai Y., Effect of blending calcium compounds on hydrolytic  
248 degradation of poly (-lactic acid-co-glycolic acid), *Biomater.*, 2002; **23**: 2479-83.
- 249 6. Kokubo T. and Takadama H., How useful is SBF in predicting in vivo bone bioactivity,  
250 *Biomater.*, 2006; **27**: 2907-15.
- 251 7. Schiller C. and Epple M., Carbonated calcium phosphates are suitable pH-stabilising fillers  
252 for biodegradable polyesters *Biomater.*, 2003; **24**: 2037-43.
- 253 8. Weiner S., An overview of biomineralization processes and the problem of the vital effect  
254 *Mineral Geochem. Rev.*, 2003; **54**: 1-29.
- 255 9. Cao W. and Hench L.L., Bioactive materials, *Ceram. Int.*, 1996; **22**: 493-1005.
- 256 10. Rea S.M., Best S.M., and Bonfield W., Bioactivity of ceramic-polymer composites with  
257 varied composition and surface topography *J. Mater. Sci. Mater. Med.*, 2004; **15**: 997-  
258 1005.
- 259 11. Nguyen T.P. and Lee B.T., Fabrication and characterization of bcp nano particle loaded  
260 pcl fiber and their biocompatibility, *Kor. J. Mater. Res.*, 2010; **20**: 31-39.
- 261 12. Lobo S.E. and Arinzeh T.L., Biphasic calcium phosphate ceramics for bone regeneration  
262 and tissue engineering applications *Mater.*, 2010; **3**: 815-26.

- 263 13. Nguyen T.P., Doan B.H.P., Dang D.V., Nguyen C.K., and Tran, N.Q., Enzyme-  
264 mediated in situ preparation of biocompatible hydrogel composites from chitosan  
265 derivative and biphasic calcium phosphate nanoparticles for bone regeneration, *Adv. Nat.*  
266 *Sci.: Nanosci. Nanotechnol.*, 2014; **5**: 015012.
- 267 14. Tran N.Q., Nguyen D.H., and Nguyen C.K., Tetronic-grafted chitosan hydrogel as an  
268 injectable and biocompatible scaffold for biomedical applications, *J. Biomater. Sci.*, 2013;  
269 **24**: 1636-48.
- 270 15. Venkatesana J., Pallelab R., Bhatnagara I., and Kim S.K., Chitosan-  
271 amylopectin/hydroxyapatite and chitosan-chondroitin sulphate/hydroxyapatite composite  
272 scaffolds for bone tissue engineering, *Inter. J. Biol. Macromol.*, 2012; **51**: 1033-1042.
- 273 16. Thein-Han W.W. and Misra R.D.K., Biomimetic chitosan-nanohydroxyapatite composite  
274 scaffolds for bone tissue engineering, *Acta Biomater.* 2009; **5**: 1182-97 ().
- 275 17. Pieróg M., Gierszewska-Drużyńska M., and Ostrowska-Czubenko J., Effect of ionic  
276 crosslinking agents on swelling behaviour of chitosan hydrogel membranes *Polish Chitin*  
277 *Society*, 2009; 75-82.
- 278 18. Cheng X., Li Y., Zuo Y., Zhang L., Li J., and Wang H., Properties and in vitro biological  
279 evaluation of nano-hydroxyapatite/chitosan membranes for bone guided regeneration,  
280 *Mater. Sci. Eng. C*, 2009; **29**: 29-35.
- 281 19. Zhang L., Li Y., Yang A., Peng X., Wang X., and Zhang X., Preparation an in vitro  
282 investigation of chitosan/ nano-hydroxyapatite composite used as bone substitute  
283 materials, *J. Mater. Sci.: Mater. Med.*, 2005; **16**: 213-219.
- 284 20. Ding S.J., Preparation and properties of chitosan/calcium phosphate composites for bone  
285 repair, *Dent. Mater. J.*, 2006; **25**: 706-712.
- 286 21. Muzzarelli R.A.A., Chitosan composites with inorganics, morphogenetic proteins and  
287 stem cells for bone regeneration, *Carbohydr. Polym.*, 2011; **83**: 1433-1445.
- 288 22. Ciapetti G., Ambrosio L., Savarino L., Granchi D., Cenni E., Baldini N., Pagani S.,  
289 Guizzardi S., Causa F., and Giunti A., Osteoblast growth and function in porous poly e-  
290 caprolactone matrices for bone repair: a preliminary study, *Biomater.*, 2003; **24**(21): 3815-  
291 3824.
- 292 23. Pan H., Zhao X., Darvell B.W., Lu W.W., Apatite formation ability- predictor of  
293 “bioactivity”?, *Acta Biomater.*, 2010; **6**: 4181-4188.
- 294 25. Mohamed K.R., El-Rashidy Z.M., Salama A.A., In vitro properties of nano-  
295 hydroxyapatite/chitosan biocomposites, *J. Ceram. Int.*, 2011; **37**: 3265.

- 296 26. Zadpoor A.A., relationship between in vitro apatite-forming ability measured using  
297 simulated body fluid and in vivo bioactivity of biomaterials, *Mater. Sci. Eng. C*, 2014; **35**:  
298 134-43.